Atomic-scale observation of the grain-boundary structure of Yb-doped and heat-treated silicon nitride ceramics

A. Ziegler[a)]
Materials Sciences Division, Lawrence Berkeley National Laboratory, Berkeley, California 94720, USA

M. K. Cinibulk
Air Force Research Laboratory, Wright-Patterson Air Force Base, Ohio 45433, USA

C. Kisielowski
Lawrence Berkeley National Laboratory, Berkeley, California 94720, USA

R. O. Ritchie[b)]
Lawrence Berkeley National Laboratory, Berkeley, California 94720, USA and Department of Materials Science and Engineering, University of California, Berkeley, California 94720, USA

(Received 18 May 2007; accepted 3 September 2007; published online 2 October 2007)

The effect of secondary sintering additives and/or a post-sintering heat treatment on the semicrystalline atomic structure of the intergranular phase in silicon nitride ceramics is investigated. Three different Yb-doped Si_3N_4 ceramic compositions are examined using a scanning transmission electron microscope, whereby the intergranular atomic structure is directly imaged with Ångstrom resolution. The resulting high-resolution images show that the atomic arrangement of the Yb takes very periodic positions along the interface between the intergranular phase and the matrix grains, and that a postsintering 1250 °C heat treatment, as well as a change of the secondary sintering additives (Al_2O_3 vs SiO_2), does not alter the atomic positions of Yb. This result has implications for the understanding of how the mechanical properties of ceramics are influenced by the presence of the nanoscale intergranular phase, and for associated computational modeling of its precise role and atomic structure. [DOI: 10.1063/1.2789390]

The variety of sintering additives for silicon nitride ceramics is relatively large, with many explored extensively over the last few decades. A group of additives that is of particular interest are the rare-earth oxides (RE_2O_3), because of their beneficial effect on microstructure development and resulting mechanical behavior.[1–9] The properties of these advanced ceramics are controlled primarily by the very thin grain boundaries (~1 nm in thickness), which surround every Si_3N_4 grain, their atomic structure and chemical composition being critical parameters.[10–13] Although chemical composition at such atomic scales can now be readily assessed using a variety of analytical methods including energy dispersive spectroscopy and electron energy loss spectroscopy (EELS),[13–16] little is known about the atomic structure of these thin intergranular films (IGFs).

At the macroscopic level, it is well documented that a variation in the type and composition of the rare-earth sintering additives results in different mechanical properties of Si_3N_4 ceramics at both room and elevated temperatures.[4,6,9,17–20] Mechanistically, the fracture process at room temperature depends on the critical flaw size/shape and the IGF, the first to allow crack initiation and the latter to control crack propagation. The IGFs strength is controlled by its chemical composition and its presence dictates whether a more transgranular or a more intergranular fracture mode ensues. However, it is also known that postsintering heat treatments can affect the macroscopic mechanical properties significantly by slightly changing the chemical composition of the IGF at the local level via diffusion and relocation of atoms and possibly by a concomitant structural transformation,[15] therefore affecting the chemical bonding strength.[4,9,21–24]

Previous studies in a similar material showed that postsintering heat treatment could cause a reduction (by ~15%) in strength.[9] adding Al_2O_3 increased the bending strength by ~6%, whereas combining Al_2O_3 with CaO caused it to decrease by ~9%.[9]

Recently, high-resolution electron-microscopy investigations into the grain-boundary structure of RE_2O_3-doped Si_3N_4 ceramics have focused on examining these atomic structures.[25–29] Results have shown how the positioning of the atoms along the interface indicates a very periodic structure, depending on atom size and electronic configuration.[25–28]

However, one pertinent question that remains is how this atomic scale information relates to macroscopic behavior, in particular the mechanical properties of the ceramic material. Specific unanswered questions that remain are (i) whether it is just the different atomic positions of the rare-earth ions and their bonding characteristics that affect the atomic bonding along the IGF and the consequent mechanical response, and (ii) the role of the surrounding structural network of silicon, nitrogen, and oxygen atoms. Undoubtedly, differing ionic structures will influence the oxygen and nitrogen incorporation and bonding along the IGF. Nevertheless, one particular question that arises is whether the rare-earth atom attachment to the interface changes after heat treatment. A further issue is that since these rare-earth oxides are usually combined with smaller quantities of other oxides, e.g.,

[a)]Present address: Max-Planck Institute for Biochemistry, Molecular Structural Biology, 82152 Martinsried, Germany.
[b)]Author to whom correspondence should be addressed. Electronic mail: roritchie@lbl.gov

Al_2O_3, SiO_2, MgO, and CaO, to form a sintering additive mixture, how do the secondary additives affect the rare-earth atom positioning, the resulting bonding characteristics and consequently the mechanical properties.

The focus of this investigation is to employ ultrahigh-resolution electron microscopy techniques to examine structural differences at the atomic level in the thin grain boundaries, specifically to address two questions: (i) how do the IGFs change after heat treatment, and (ii) how does an additional sintering additive affect rare-earth attachment.

Silicon nitride samples were fabricated via a two-step gas-pressure-sintering technique, ensuring a high-purity material. The rare-earth oxide additive used for the material examined in this study is Yb_2O_3. A total of three samples were investigated. The first material composition (hereafter sample 1) was prepared with 5 vol % Yb_2O_3+0.5 vol % Al_2O_3.[10] Sample 2 had the same nominal composition but after densification it was heat treated at 1250 °C under 0.1 MPa N_2 for 12 h.[10] Sample 3 was the second material composition and was prepared with 6.1 vol % Yb_2O_3 and 6.7 vol % SiO_2, for a 1:2 molar ratio.[3] After densification it was heat treated at 1400 °C under 1.4 MPa N_2 for 24 h. Although prepared with different compositions, the resulting microstructures of all three samples resemble those of numerous other Si_3N_4 microstructures, i.e., they exhibit elongated matrix grains of sizes between 0.4 and 4 μm with aspect ratios of ~8–10. The grains were surrounded by the grain-boundary phase, including the commonly formed ytterbium disilicate phase at the grain triple junctions and the thin intergranular film that is of interest in this investigation. Although there were three different processing conditions, EELS analysis was performed only on the two different compositions; the purpose here was only to confirm the presence of Al in samples 1 and 2. The much more essential scanning transmission electron microscopy (STEM) investigations were conducted on all three conditions. All samples were prepared via the standard transmission electron microscopy (TEM) sample preparation techniques, namely, grinding, dimpling, and ion-beam milling.

Experimental EELS and high-resolution *Z*-contrast images were obtained employing STEM (FEI Tecnai F20 STEM), operating at similar imaging and spectroscopy settings as in previous studies.[25,27]

High-resolution STEM images (raw and unfiltered), shown in Fig. 1, depict the atomic interface between a Si_3N_4 matrix grain, oriented along the low-index zone axis [0001], and the vitreous intergranular phase. Figure 2 presents the supporting compositional EELS analysis. Multiple spectra were acquired for each sample composition; however, for simplicity reasons only two spectra (called spec1 and spec2) of each sample (1 and 3) are shown in Fig. 2. A direct comparison of the background subtracted, energy-loss spectra clearly demonstrates that the interface in the $Yb_2O_3+Al_2O_3$ sample (1) contains Al, while the $Yb_2O_3+SiO_2$ sample (3) does not. The Al-$L_{2,3}$ edge is located at 73 eV while the Si-$L_{2,3}$ edge is at 99 eV. After background subtraction in both spectra of samples 1 and 3, the Si-$L_{2,3}$ edge can be identified (all spectra are normalized to the Si-$L_{2,3}$ peak); however, the Al edge can only be detected in the spectrum of the $Yb_2O_3+Al_2O_3$ sample (1). The Si signal is strong in both materials because the entire Si_3N_4 matrix contains Si and influences the EELS analysis. Nevertheless, Al is only predominantly present along the grain boundaries as it usually does not substitute for Si in the Si_3N_4 matrix phase.

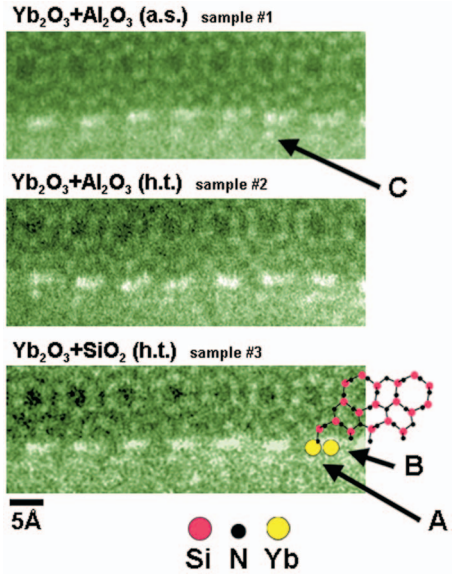

FIG. 1. (Color) High-resolution STEM images depicting the interface between Si_3N_4 matrix and the intergranular phase. The Yb atoms, visible here as bright spots due to enhanced electron scattering, are located periodically along the interface at distinct atomic positions A, B, and C.

The spatial resolution in the STEM is 1.4 Å, and as such the individual close atomic positions of Si–N cannot be fully resolved. However, from previous studies using phase-reconstruction microscopy techniques, it is well known that the observed hexagonal ring structures represent the typical Si_3N_4 atomic structure.[27,30,31] The *Z* contrast in the STEM images (Fig. 1) allows direct identification of the Yb atoms within the thin intergranular phase. Ytterbium is a relatively heavy element (Z=70) and thus it scatters the incoming electrons in the microscope more strongly than silicon or nitrogen atoms. Hence, the atomic positions of Yb become visible in the STEM image as bright spots along the interface. Note that the positions of these bright spots do not coincide with any atomic position of the Si_3N_4 crystal structure (even if it were to be theoretically extended into the grain-boundary phase). Yb atoms do not substitute for Si_3N_4 host atoms in

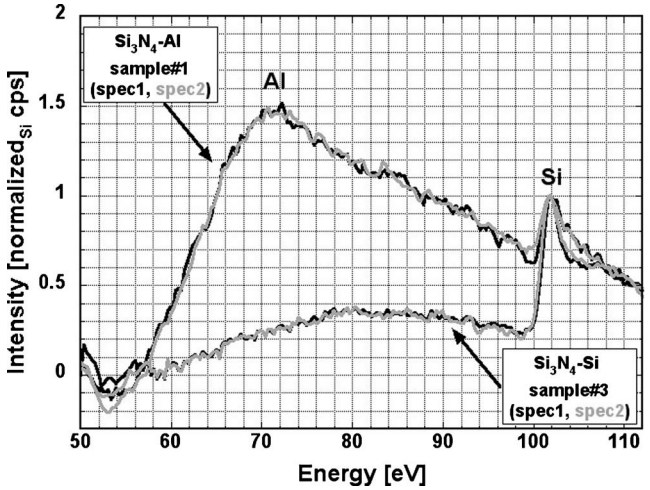

FIG. 2. EELS analysis spectra clearly revealing the presence of Al in the grain boundaries in $Yb_2O_3+Al_2O_3$ sample 1 along the intergranular phase, which is not present in $Yb_2O_3+SiO_2$ sample 3: The characteristic Al-$L_{2,3}$ peak is at 73 eV.

their atomic positions nor do they reside on interstitial sites in the Si_3N_4 crystal structure. Yb atoms, as well as other elements, segregate to the intergranular phase where they can be identified chemically by EELS.[25,27,29] As a result, the bright spots in the STEM image represent a distinctly different atomic structure with a periodic arrangement of Yb atoms. The Yb atoms bond in atom-pair configuration, A and B (see Fig. 1), which is a characteristic feature of the heavier, but smaller lanthanide elements ($Z > Z_{Sm}$).[25] The atom-pair axis is oriented parallel to the prismatic plane; however, it cannot be determined to what degree the axis is also parallel to the image plane. Nevertheless, observing how close the bright spots are and considering the atomic size of these elements, it follows that the atom-pair axes must be inclined and are seen in projection. The average atom-pair separation (in projection) of Yb can be determined to 1.46 ± 0.05 Å ($Yb_2O_3 + Al_2O_3$ sample 1), 1.47 ± 0.04 Å (heat-treated $Yb_2O_3 + Al_2O_3$ sample 2), and 1.45 ± 0.05 Å ($Yb_2O_3 + SiO_2$ sample 3). These atom separations were each determined by averaging over approximately 30 atomic distance of interest. Upon close examination of the STEM images though, one can recognize occasional pair splitting, i.e., some atom pairs appear to be separated more than others. This appears to occur in all three samples examined. Furthermore, one can discern additional bright spots at position C (see Fig. 1). This position is closest to position A but further away from the Si_3N_4 matrix grain interface, perpendicular to the A-B atom-pair axis, i.e., extending the semicrystalline atomic structure of Yb atoms and reaching into the grain-boundary phase.

The most important finding of this STEM investigation is that in all three samples, the atom positions of the Yb atoms do not change within the margin of experimental error (0.05 Å) and are independent of the secondary sintering additives and thermal history. This finding is of paramount importance as it demonstrates that the primary sintering elements, often lanthanides, cannot be solely responsible for changes in fracture behavior of the ceramic material. Their atomic positions do not change as one would expect when these elements are allowed to diffuse and/or relocate to energetically more favorable atomic positions along the grain boundaries during heat treatment. Surprisingly, they also seem not to change when a completely different secondary sintering aid element is added (here Al_2O_3). The constancy of the Yb atomic positions is a strong indicator that something else, e.g., possibly the secondary sintering aid elements and/or the nitrogen to oxygen ratio, must be of equal or higher importance for the changes in mechanical properties following heat treatment or differences in the secondary sintering aid elements. A change in the Yb-surrounding grain-boundary chemistry would be expected to also alter the atomic positions of the Yb atoms relative to the Si_3N_4 matrix structure, especially since the valence and bonding characteristics change. However, as seen in Fig. 1, this is not supported by our experimental observations. Unfortunately, the atomic positions of such secondary sintering aid elements (Al, O) cannot be distinguished from elements close in atomic number (Si=14, Al=13, O=8, N=7).

In conclusion, based on an experimental Ångstrom-resolution STEM study of grain-boundaries in Yb-doped silicon nitrides, the presented experimental images do not reveal any major change or shift in atomic position of the primary sintering additive cations, Yb, in the boundary following 1250 °C heat treatment or the addition of a secondary sintering aid (Al_2O_3), although the individual Yb atoms and their respective atomic positions along the Si_3N_4 grain-boundaries can be clearly identified in all samples.

This work was supported by the Director, Office of Science, Office of Basic Energy Sciences, Division of Materials Sciences and Engineering, of the U.S. Department of Energy under Contract No. DE-AC02-05CH11231.

[1] H. J. Kleebe and M. K. Cinibulk, J. Mater. Sci. Lett. **12**, 70 (1993).
[2] E. Y. Sun, P. F. Becher, K. P. Plucknett, C. H. Hsueh, K. B. Alexander, S. B. Waters, K. Hirao, and M. E. Brito, J. Am. Ceram. Soc. **81**, 2831 (1998).
[3] M. K. Cinibulk, G. Thomas, and S. M. Johnson, J. Am. Ceram. Soc. **75**, 2037 (1992).
[4] M. K. Cinibulk, G. Thomas, and S. M. Johnson, J. Am. Ceram. Soc. **75**, 2050 (1992).
[5] W. A. Sanders and D. M. Mieskowski, J. Am. Ceram. Soc. **64**, 304 (1985).
[6] M. J. Hoffmann, in *Tailoring of Mechanical Properties of* Si_3N_4 *Ceramics*, edited by M. J. Hoffmann and G. Petzow (Kluwer, Netherlands, 1994), pp. 59–72.
[7] C. M. Wang, X. Pan, M. J. Hoffmann, R. M. Cannon, and M. Rühle, J. Am. Ceram. Soc. **79**, 788 (1996).
[8] D. R. Clarke, J. Am. Ceram. Soc. **70**, 15 (1987).
[9] M. J. Hoffmann, in *Tailoring of Mechanical Properties of* Si_3N_4 *Ceramics*, edited by M. J. Hoffmann and G. Petzow (Kluwer, Netherlands, 1994), pp. 233–243.
[10] H. J. Kleebe, M. K. Cinibulk, R. M. Cannon, and M. Rühle, J. Am. Ceram. Soc. **76**, 1969 (1993).
[11] H. J. Kleebe, M. J. Hoffmann, and M. Rühle, Z. Metallkd. **83**, 610 (1992).
[12] I. Tanaka, H. J. Kleebe, M. K. Cinibulk, J. Bruley, D. R. Clarke, and M. Rühle, J. Am. Ceram. Soc. **77**, 911 (1994).
[13] H. J. Kleebe, J. Bruley, and M. Rühle, J. Eur. Ceram. Soc. **14**, 1 (1994).
[14] H. Gu, X. Pan, R. M. Cannon, and M. Rühle, J. Am. Ceram. Soc. **81**, 3125 (1998).
[15] A. Ziegler, J. M. McNaney, M. J. Hoffmann, and R. O. Ritchie, J. Am. Ceram. Soc. **88**, 1900 (2005).
[16] H. Gu, Mater. Trans. **45**, 2091 (2004).
[17] P. F. Becher, S. L. Hwang, and C. H. Hsueh, MRS Bull. **20**, 23 (1995).
[18] S. M. Wiederhorn, Annu. Rev. Mater. Sci. **14**, 373 (1984).
[19] P. F. Becher, J. Am. Ceram. Soc. **74**, 255 (1991).
[20] F. F. Lange, B. I. Davis, and D. R. Clarke, J. Mater. Sci. **15**, 601 (1980).
[21] F. F. Lange, B. I. Davis, and D. R. Clarke, J. Mater. Sci. **15**, 616 (1980).
[22] F. F. Lange, B. I. Davis, and M. G. Metcalf, J. Mater. Sci. **18**, 1497 (1983).
[23] M. J. Hoffmann, MRS Bull. **20**, 28 (1995).
[24] M. Backhaus-Ricoult and Y. G. Gogotsi, J. Mater. Res. **10**, 2306 (1995).
[25] A. Ziegler, J. C. Idrobo, M. K. Cinibulk, C. Kisielowski, N. D. Browning, and R. O. Ritchie, Science **306**, 1768 (2004).
[26] G. B. Winkelmann, C. Dwyer, T. S. Hudson, D. Nguyen-Manh, M. Doblinger, R. L. Satet, M. J. Hoffmann, and D. J. H. Cockayne, Philos. Mag. Lett. **84**, 755 (2004).
[27] A. Ziegler, J. C. Idrobo, M. K. Cinibulk, C. Kisielowski, N. D. Browning, and R. O. Ritchie, Appl. Phys. Lett. **88**, 041919 (2006).
[28] C. Dwyer, A. Ziegler, N. Shibata, G. B. Winkelmann, R. L. Satet, M. J. Hoffmann, M. K. Cinibulk, P. F. Becher, G. S. Painter, N. D. Browning, D. J. H. Cockayne, R. O. Ritchie, and S. J. Pennycook, J. Mater. Sci. **41**, 4405 (2005).
[29] N. Shibata, S. J. Pennycook, T. R. Gosnell, G. S. Painter, W. A. Shelton, and P. F. Becher, Nature (London) **428**, 730 (2004).
[30] A. Ziegler, C. Kisielowski, and R. O. Ritchie, Acta Mater. **50**, 565 (2002).
[31] A. Ziegler, C. Kisielowski, and R. O. Ritchie, J. Am. Ceram. Soc. **86**, 1777 (2003).